NJC

Accepted Manuscript

This is an *Accepted Manuscript*, which has been through the Royal Society of Chemistry peer review process and has been accepted for publication.

Accepted Manuscripts are published online shortly after acceptance, before technical editing, formatting and proof reading. Using this free service, authors can make their results available to the community, in citable form, before we publish the edited article. We will replace this *Accepted Manuscript* with the edited and formatted *Advance Article* as soon as it is available.

You can find more information about *Accepted Manuscripts* in the Information for Authors.

Please note that technical editing may introduce minor changes to the text and/or graphics, which may alter content. The journal's standard Terms & Conditions and the Ethical guidelines still apply. In no event shall the Royal Society of Chemistry be held responsible for any errors or omissions in this *Accepted Manuscript* or any consequences arising from the use of any information it contains.

ROYAL SOCIETY OF CHEMISTRY

www.rsc.org/njc

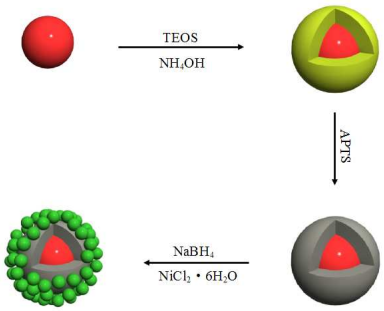

The synthesis of hierarchical nickel anchored on Fe_3O_4@SiO_2 has been demonstrated and their successful utilization to remove the abundant proteins(BHb) in bovine blood.

Cite this: DOI: 10.1039/c0xx00000x

www.rsc.org/xxxxxx

ARTICLE TYPE

The synthesis of hierarchical nickel anchored on Fe_3O_4@SiO_2 and its successful utilization to remove the abundant proteins (BHb) in bovine blood have been demonstrated

Yongtao Wang†, Min Zhang†, Linlin Wang†, Weizhen Li†, Jing Zheng†, Jingli Xu†**

Received (in XXX, XXX) Xth XXXXXXXXX 20XX, Accepted Xth XXXXXXXXX 20XX
DOI: 10.1039/b000000x

A hierarchical nickel shell anchored on silica coated magnetic Fe_3O_4@SiO_2 nanospheres (MNPs) has been designed and constructed that combined the capacity of effective adsorption for protein bovine hemoglobin (BHb) and selective deletion BHb from the bovine blood real sample. Firstly, -NH_2 modified silica/ magnetite nanoparticles (Fe_3O_4@SiO_2-NH_2) were synthesized by the combination of a sol–gel method and refluxing process. The Fe_3O_4@SiO_2-NH_2 composites revealed a core-shell structure, and the thickness of silica shell can be easily adjusted by controlling the amount of ammonium solution. Then, hierarchical nickel shell were anchored on the surface of Fe_3O_4@SiO_2-NH_2 by reducing Ni^{2+} between the Fe_3O_4@SiO_2-NH_2 solid and nickel solution with $NaBH_4$. By taking advantages of the high affinity of Ni^{2+} on the shell surface toward His-tagged proteins and the fast response toward an assistant magnet, the hetero-nanoparticles can be applied to selectively bind to and magnetically separate of BHb from the bovine blood. Significantly, it is expected that this approach can be extended to other bimolecular separation and purification.

1. Introduction

Magnetic nanoparticles have been extensively studied due to their unique magnetic properties and potential applications in the frontier fields of data storage technology, environmental and bio molecular separation, magnetic resonance imaging, drug delivery, enzyme immobilization, and immunoassays. [1–7] They have also found a wide range of applications in the enrichment of proteins and peptides in proteomics research.[8-9] To apply magnetic nanoparticles in proteomics applications, much work has been done to functionalize magnetic nanoparticles surface with another phase to enhance the compatibility and functionality. Such functionalized magnetic nanoparticles can be a versatile platform for effective manipulation of various kinds of proteins, which is important in the field of proteomics. Since inorganic(e.g. silica) or organic(polymer) shell can protect the magnetic particles from magnetic dipolar interactions, it has been exploited as a coating material for functionalization magnetic nanoparticles. This capability allows for magnetic carriers that can be used for nucleic acid separation,[10] enzyme immobilization,[11] However, the significant decrease of magnetization, stemmed from the silica or polymer shell in the core/shell structure, can lead to the difficulty of magnetic separation, which is a disadvantage for application in fields using magnetization. Therefore, it is essential to seek a novel coating method for synthesizing magnetic multifunctional composites with stronger magnetization while endowing with the functionality.

Immobilized metal affinity (IMA) separation on magnetic matrix is based on the selective interaction between the electron donor groups on the proteins and on the transition-metal ions [Cu(II), Ni(II), Zn(II), or Co(II)] which are loaded on the chelating ligands coupled to magnetic support. Among the transition metal ions, the nickel ion has been widely used in the successful application to the magnetic separation of proteins. A variety of nickel anchored magnetic nanomaterials were recently developed for enriching peptides and proteins based on their strong magnetic properties, facilitating the rapid and convenient isolation of nanomaterial–target peptide/protein complexes from the sample solution.[12–19] These materials were mainly prepared by assembling a variety of organic or inorganic materials on magnetic iron oxide particles followed by chemical modification and surface coating. Kim et al designed a magnetically recyclable protein separation system by combining ferrimagnetic magnetite cores and NiO nanoparticles decorated onto a mesoporous silica shell with a high surface area. The exposed NiO nanoparticles provide for a selective adsorption of His-tagged protein from the mixed-protein solution. [14] On the similar principle, nickel-doped magnetite, NiO-decorated MNPs, and nickel silicate-coated magnetic heterostructures have also been developed.[16-19] Chen and coworkers have reported a serials of methods to synthesize iminodiacetic acid (IDA) immobilized MNPs, and then charged with Cu^{2+} or Ni^{2+} for selective capture of His-rich bovine hemoglobin (BHb).[20-24] Wang and Zheng group have synthesized nickel immobilized Fe_3O_4@Polymer to enrich the His-tagged protein protein.[25-27] These systems, however, still suffer from drawbacks such as low magnetic response, complicated synthesis routes, and severe aggregation of nanomaterials. Furthermore, the functional group shell can also lead to the decrease of magnetism.

As an important magnetic material, nickel-based nanomaterials have been successfully synthesized by using a variety of approaches.[28–29] The nickel metal was not only used for magnetic support, but also can enrich the histine protein with the specific metal affinity to polyhistidine groups. Mirkin and co-workers demonstrated the efficient and selective separation of His-tagged proteins using Ni containing magnetic nanorods with a diameter of about 300 nm.[30] Hyeon etc have further developed NiO coated Ni nanoparticles as a novel agent to bind and magnetically separate histidine-tagged (His-tagged) proteins.[31] Recently, Wang group have synthesized the

graphene–nickel (GP–Ni) hybrid to selective isolate/purify His6-tagged recombinant proteins from cell lysate.[32] Another graphene–Ni hybrid was also prepared for enrichment and identification of proteins and peptides.[33] This inspired us to evaluate whether such a nickel coating could be applied to magnetic nanoparticles to realize the target of both increasing magnetism and adsorbing protein. The following experimental results are in good agreement with our expectation. To functionalize the magnetic nanoparticles, silica was also selected as a good candidates being the coating materials. In addition to protect the magnetic particles from leaching in an acid environment, silica owns other obvious advantages as follows. (1) the silica coating may make them biocompatible, which is gentle to the biomacromolecules such as protein and DNA (2) it provides them with a silica-like surface and easily modified with various groups. Although the silica coating decreases the magnetism of the functional composites, the following immobilized nickel shell can make up for the loss of magnetism. In this study, we present a simple pathway to synthesize magnetic silica microspheres with coated nickel shell for fast and efficient removal of abundant protein(BHb) in bovine blood. First, magnetite silica microspheres were synthesized and modified with NH_2 groups, Fe_3O_4@SiO_2@NH_2 was coated with Ni metal via reduced by $NaBH_4$ in aqueous solution, leading to Ni-immobilized magnetite silica microspheres (donated as Ni-MNs). Since the Ni-MNs possess high specific area and strong magnetism, they can be readily separated from their dispersion or mixture solution containing analytes with the assistance of an external applied magnetic field, thus achieving efficient removal of the targeted species. By virtue of the unique magnetic responsivity of magnetite and the trapping ability of the immobilized nickel shell, we have successfully removed the abundant protein(BHb) in bovine blood.

2. Experimental Section

2.1 Chemicals

Isopropanol, polyvinyl pyrrolidone (PVP), ferric chloride hexahydrate ($FeCl_3 \cdot 6H_2O$), isopropanol, 3-aminopropyl-triethoxysilane (APTS), and sodium borohydride were purchased from Shanghai Lanji Co. Ltd. (Shanghai, China). Other reagents were of analytical grade or better and used without further purification. Deionized water was prepared with a Milli-Q water purification system (Millipore, Milford, MA).

2.2 Synthesis of $NH_2/SiO_2/Fe_3O_4$ composite nanoparticle

Fe_3O_4 spheres with high saturation magnetization were synthesized by a polyol media solvothermal method according to reference with some modifications. For the coating of silica spacer on the Fe_3O_4 core, a certain amount of synthesized Fe_3O_4 spheres were dispersed in a mixture of 140 mL isopropanol, 10 mL water and 2 mL of aqueous ammonia in a round bottomed flask by ultrasonic agitation for 15 min. Then 1 g of PVP was added with gentle stirring at room temperature for 6 h. After washing with ethanol, the particles were transferred into a mixture of isopropanol (50 mL) and 3-aminopropyl-triethoxysilane (APTS, 800 uL) and heated up to 80°C for 2 hours to functionalize the silica surface with amino groups. The $–NH_2$ terminated Fe_3O_4/SiO_2 colloids were washed with isopropanol and dispersed back in de-ionized water.

2.3 Preparation of Ni/ $NH_2/SiO_2/Fe_3O_4$

5 mL aqueous solution of $NaBH_4$ (100 mg) was added to an aqueous suspension containing 250 mg $–NH_2$ terminated Fe_3O_4/SiO_2 colloids and 500 mg of $Ni(NO_3)_2$ and mechanically stirred at room temperature for 24 hours. Resulting solid of Ni-MNP was isolated by magnetic decantation and purification process was repeated three times by addition of water, ethanol respectively.

2.4 Instrumentation

The Scanning electron microscopy (SEM,Shimadzu, Japan) and a transmission electron microscope (TEM) were used to characterize the microscopic features of the samples. Fourier transform infrared (FT-IR) spectra (4000-400 cm^{-1}) in KBr were recorded using the AVATAR 360 FT-IR spectrophotometer (Nicolet, Waltham, USA). The data of UV-vis adsorption were obtained by using UV-2450 spectrophotometer (Shimadzu, Japan). The crystal structure of nanoparticles was determined by X-ray diffractometer (XRD). The XRD pattern of each sample was recorded with a Shimadzu (Japan) D/Max-2500 diffractometer, using a monochromatized X-ray beam with nickel-filtered Cu Kα radiation. The XRD patterns were collected in the range of $5° < 2\theta < 80°$ with a dwelling time of 2s and a scan rate of 6.0°/min. The substance is automatically searched by using JCPDS-International Center for Diffraction Data. The X-ray photoelectron spectrometric (XPS) spectra were obtained on a Shimadzu (Japan) Kratos AXIS Ultra DLD X-ray photoelectron spectrometer with an Mg Kα anode (15kV, 400W) at a takeoff angle of 45°. The source X-ray was not filtered, and the instrument was calibrated against the C1s band at 285eV. The size and morphology of the nanoparticles were measured by a FEI (Netherlands) Tecnai-20 Transmission Electron Microscopy. Magnetic properties were measured with a LDJ9600-1 (U.S. A.) vibrating sample magnetometer at room temperature.

3. Results and Discussion

3.1 Synthesis and Characterization of $Ni/NH_2/SiO_2/Fe_3O_4$ NPs composite material

The strategy for synthesizing Fe_3O_4@SiO_2@NH_2–Ni(Ni-MNP) microspheres is schematically depicted in Scheme 1.The morphology of the resulting product was investigated by scanning electron microscopy (SEM) and transmission electron microscopy(TEM). Fig 1a, 1b shows the typical SEM image of the as-prepared Fe_3O_4 NPs with different magnification, As shown, the silicon substrate is fully covered with Fe_3O_4 spheres that have a relatively narrow size distribution. From the TEM analysis, these particles have a mean diameter 350 nm(Fig.1c). We also investigate that the influence of the size of Fe_3O_4 by adding different amount of PVP, it is indicated the amount of the PVP has obvious influence on the size of the Fe_3O_4. With the increasing the amount of PVP from 1 g to 3 g, the size of Fe_3O_4 grow more bigger(Fig. 1(c-e)), and when the PVP amount is 2 g, the morphology of Fe_3O_4 is nearly monodisperse(Fig. 1d). The diameters of Fe_3O_4 cores can also be tuned in the range of 100–1500 nm by carefully controlling the other solvothermal parameters, such as the holding temperature and time, concentration of reactants, as Li etc reported.[34] In the present approach, PVP participated in the hydrothermal reaction to prevent against particle agglomeration as a stabilizer or surfactant, what's more important, due to the coordination of PVP, the PVP may be adsorbed onto the magnetic microspheres, which is verified on FTIR, the C=O of PVP is red-shifted from 1675 cm^{-1} to 1643 cm^{-1}[data not shown], this will contribute to silica coating on magnetic microspheres in the following experiment.[15,16]

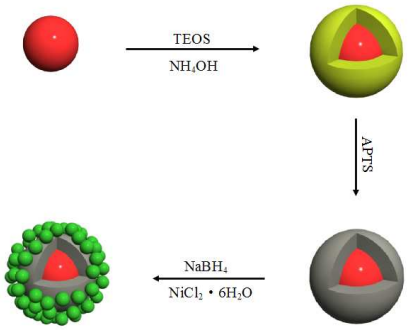

Scheme 1 the procedure of hybrid Ni-MNP microspheres

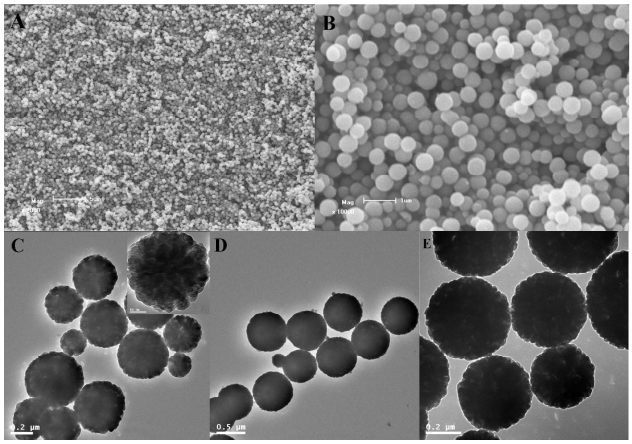

Fig. 1 (a-b) SEM image of the as-prepared Fe_3O_4 microspheres with increasing magnification (c-e) TEM images of the as-prepared Fe_3O_4 microspheres composite with increasing addition of PVP. Note the scale bar.

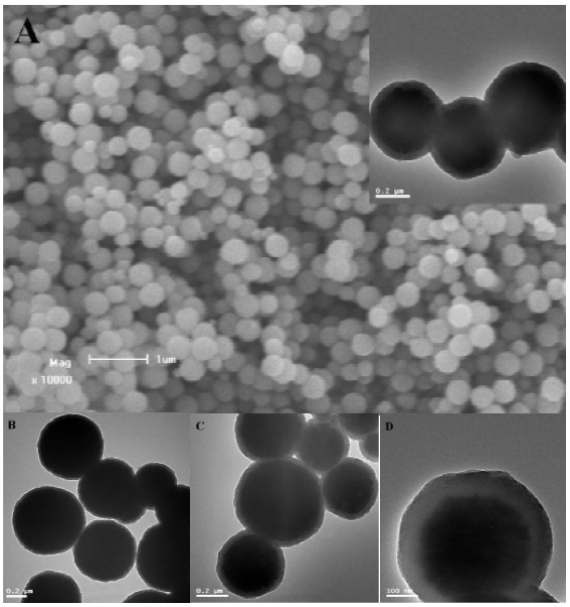

Fig. 2(a) display the SEM and TEM imagine of Fe_3O_4@SiO_2 (b) to (d) show the Fe_3O_4@SiO_2 under different conditions varing the NH_3 amount (c) 1mL (d) 2mL (e) 3mL

There have been several reports of the direct coating of magnetic nanoparticles with silica. For magnetic oxide in particular, no primer was required to promote the deposition and adhesion of the silica shell under certain conditions, because the iron oxide surface has a strong affinity toward silica. In the work reported herein, the PVP is necessary. PVP plays dual role in the sol-gel reaction. First it stabilize the Fe_3O_4 in order to circumvent the sendimentation, ensure to obtain well-dispersed spherical composite particles, second it also contribute to the encasulation of Fe_3O_4@SiO_2.

The morphology of Fe_3O_4@SiO_2 particles is characterized by TEM. It is found that the outer shell of the particle exhibits a fine increment in brightness compared with the dark inner core, which confirms the well-known core-shell structure of Fe_3O_4@SiO_2 particles, where Fe_3O_4 is the magnetic core embedded within the silica matrix. It is noted that the SiO_2 shell structured Fe_3O_4@SiO_2 particles are rather well-dispersed, determined by TEM are 20, 50 and 75 nm, the silica shell thickness of the nanoparticles increase with increasing the aqueous ammonia from 1 mL to 3 mL. This observation clearly demonstrates that the nanoparticle characteristics of Fe_3O_4@SiO_2 nanoparticles can be easily controlled by simply varying the initial amount of NH_3, it is also easily controlled by the TEOS, the reaction time. Due to the presence of negative charges on the surfaces of silica shells, these magnetic nanoparticles having a core-shell structure could form very stable dispersions in water without adding other surfactants, which facilitate the reaction in aqueous solution.

The magnetite microspheres were coated with silica for the purpose of preventing the magnetite aggregation and easily functionalized. The surface of magnetic silica is biocompatible and can be functionalized with the silane coupling agent. In order to provide the surface with the ability to bind nickel ion, (3-aminopropyl)triethoxylsilane (APTES) were covalently bound to the surface of magnetic silica microspheres, The assembly of Ni nanoparticles on the silica surface was carried out by incubating the Ni^{2+} solution and amine-functionalized silica particles and reaction for 24 h via reduced by $NaBH_4$, the nickel shell exhibit the porous morphology, which is shown in Fig 3(A-B). Yin etc[35-36] have reported that silica sphere can be etching in an excessive NaBH4 solution. Herein in our work, the $NaBH_4$ was added to reduce the nickel ions while stirring for 24 hours. As a result, the silica shell may be etched in the process of coating nickel metal. Thus, we can not observe the tri-layer of the Ni-Fe_3O_4@SiO_2 from the TEM imagine.

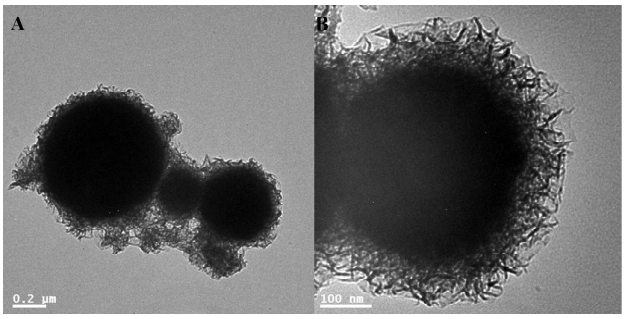

Fig. 3(A and B) display the TEM imagine of Ni-MNP at increasing magnification

Fig. 4 shows the XRD patterns of solvothermally prepared bare Fe_3O_4 particles and the Fe_3O_4/SiO_2 composite, and no other characteristic peaks due to the impurities of hematite or hydroxides were detected. In the curve (a), all the diffraction peaks can be indexed to well crystallized magnetic Fe_3O_4 (JCPDS 75–1609). It must be pointed that the magnetite (Fe_3O_4) compound in the particles may be mixed with maghemite(γ-Fe_2O_3). Because they have very similar magnetic properties, identification is not important in the present study.

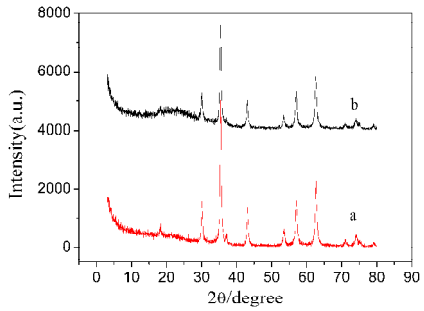

Fig. 4 XRD diffraction patterns of the as-prepared a) Fe_3O_4. b) $Fe_3O_4@SiO_2$.

XPS have been considered as a useful tool for qualitatively determining the surface component and composition of a sample. The survey and the respective element XPS of Ni-MNP are given in Fig. 5. The binding energy of Ni (3p, 516.5 eV), C1s(3d5/2, 157.1 eV), and Si(2p, 103.3 eV) is obvious. It should be noted that the binding energy of iron (Fe) can't be detected in the XPS. This may be due to the limitation of XPS analysis which can't penetrate nickel coated silica shell. The Ni 2p peaks at ~881 eV and ~873 eV are assigned to Ni 2p1/2, and at ~862 eV and ~856 eV are assigned to Ni 2p3/2, which exibits similar peaks to nickel(II) oxide[37], these result fully indicates that the presence of nickel after reduction. Based on this observation, it is proved that the deposition of metallic Ni(0) species at the iron oxide surface through the reduction by $NaBH_4$ and subsequent re-oxidation into NiO or Ni(II) species in an aqueous environment.

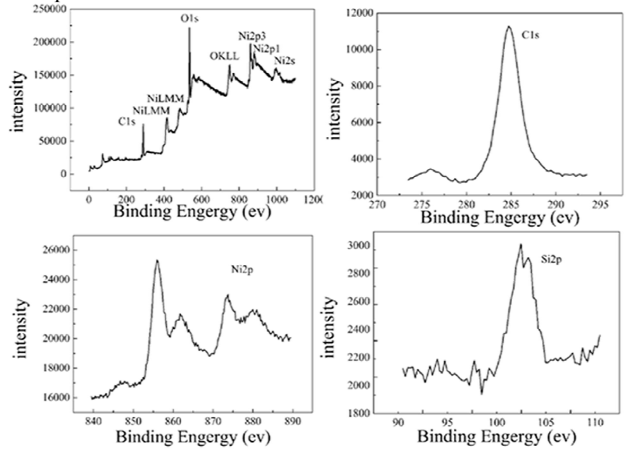

Fig. 5 XPS patterns of the Ni-MNP composite.

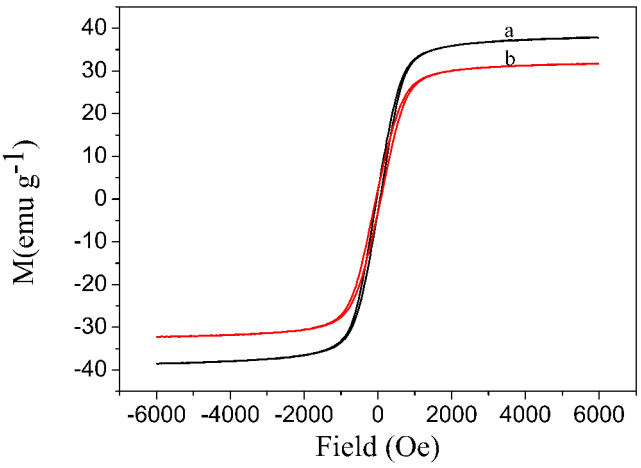

Fig. 6 Field-dependent magnetization of Ni-MNP (a), $Fe_3O_4@SiO_2@NH_2$ (b).

The hysteresis loops of the prepared samples were registered at 300K. The magnetic behaviour of the Ni-MNP was investigated using a superconducting quantum interference device (SQUID) magnetometer (Fig. 6). The saturation magnetization value of $Fe_3O_4@SiO_2@NH_2$ is 32.02 emu g^{-1}, but it increase to 38.22 emu g^{-1} for Ni-MNP, which is attributed to the immobilized nickel metal shell on the magnetic silica microspheres. Although the magnetization curves show hysteresis, the remanent magnetization values of $Fe_3O_4@SiO_2@NH_2$-Ni are very small, 2.427 emu g^{-1} for the resulting product. After dispersing the Ni immobilized magnetic silica microspheres (Ni-MNP) in water by shaking, vortexing, or sonication, they can be easily attracted within several minutes by placing a small magnet on the side of the vessel.

The nickel immobilized silica-coated magnetite sub-microspheres were tested in phosphate buffer (pH 8.0) by the batch experiment. Firstly, 10 mg of nickel immobilized silica-coated magnetite sub-microspheres were mixed with 5 mL of various concentrations of BHb solution (0.2–5.0 mg ml^{-1}). Then, the mixture was shaken at 25ºC for 12 h and the times would be sufficient to reach adsorption equilibrium. In all adsorption and elution buffers, 0.5 M NaCl was included to minimize the ion-exchange interactions. As can be seen from Fig. 7, the BHb was effectively adsorbed. The BHb adsorption isotherm could be described by the Langmuir equation:

$$q = \frac{q_m c}{K_d + c}$$

where c (mg mL^{-1}) and q (mg g^{-1}) are the aqueous protein concentration and the amount of adsorbed protein at equilibrium, respectively. q_m(mg g^{-1}) is the maximum adsorption capacity and K_d (mg mL^{-1}) is the dissociation constant. By fitting the experimental data to the Langmuir equation, q_m and K_d are estimated to be 1054.3 mg g^{-1} and 0.25 mg mL^{-1} respectively.

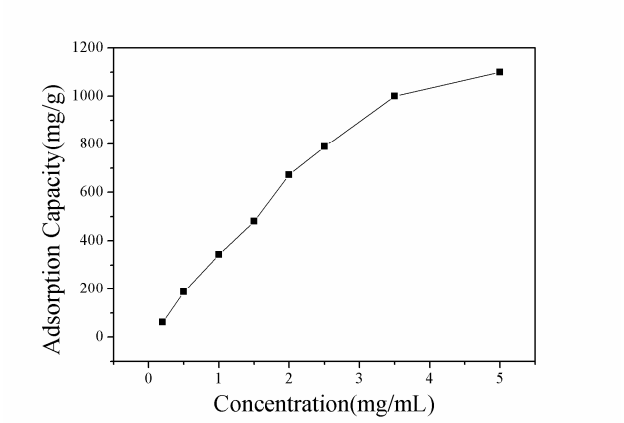

Fig. 7 Adsorption isotherm of BHb on magnetic Ni-MNP in the solution containing 20 mM phosphate and 0.5M NaCl at pH 8.0.

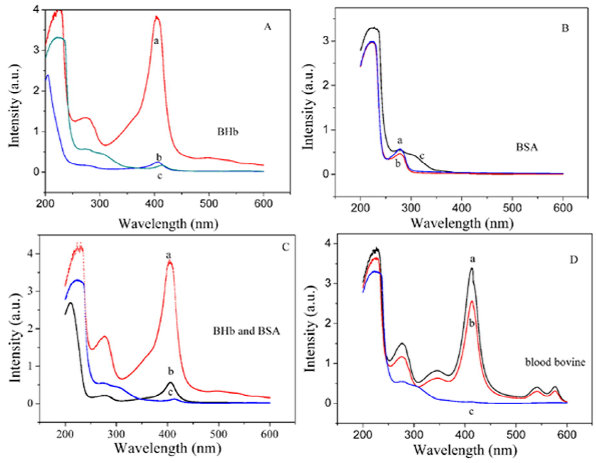

Fig. 8 Curve a is the UV-vis spectrum of 0.8 mg mL^{-1} of the BHb (A), BSA (B) BHb and BSA mixture (C), and diluted bovine blood (D) before adsorption by Ni-MNP. Curve b is the UV-vis spectrum of supernatant of above BHb (A), BSA (B), BHb and BSA mixture (C), and diluted bovine blood (D) after adsorbed by Ni-MNP. Curve c is the UV-vis spectrum of desorption solution of the adsorbed protein by Ni-MNP in BHb (A), BHb and BSA mixture (C) and diluted bovine blood (D) using concentration of 0.1 g mL^{-1} of imidazole solution as the eluent.

The efficiency of protein separation by Ni-MNP was investigated by following their reaction with BHb and BSA. It is well known that BSA and BHb are the two most abundant proteins in bovine blood, which seriously hamper the detection of less abundant proteins that are often markers of diseases. The single protein BHb (0.8 mg mL^{-1}) and BSA (0.8 mg mL^{-1}), a binary protein mixture containing 0.8 mg mL^{-1} BHb and BSA respectively, and 100-fold diluted bovine blood solution were incubated with Ni-MNP for 3 h at room temperature. Ni-MNP were separated by an external magnet and eluted by imidazole solution (0.1 g mL^{-1}). The protein concentration in the supernatant and the eluent was analyzed using a UV-vis spectrophotometer at 280 and 406 nm for BSA and BHb respectively. As shown in Fig. 8, the absorption intensity at 406 nm is greatly decreased for all protein solutions containing BHb and nearly decreased to zero for the single BHb solution (Fig. 8A). However, the adsorption intensity of BSA at 280 nm exhibits a negligible decrease (Fig. 8B). The results show the selective adsorption of BHb by Ni-MNP from the solution. The difference in the adsorption capacity of Ni-MNP towards BHb and BSA may be ascribed to the different histidine residues in the proteins. It is well known that the number of accessible histidine residues on BHb is 24, whereas there are only 2 histidine residues on the surface of BSA. In comparison with the single BHb, BHb and BSA solution, the adsorption capacity of the Ni-MNP towards BHb in the 100-fold diluted bovine blood (Fig. 8D) lessened. It was found that the adsorption of Ni-MNPs to BHb in the 0.8 mg mL^{-1} BHb and BSA binary solution and the 100-fold diluted bovine blood is higher than that of single BHb solution, respectively. The reason may be attributed to the interaction between BHb and BSA, other proteins in the bovine blood, which have a negative influence on the adsorption of BHb. The captured BHb on the Ni-MNPs was released by the treatment of the MNPs with imidazole solution (0.1 g mL^{-1}). Because the imidazole has a strong metal chelating interaction with Ni^{2+}, it resulted in the release of BHb protein from the Ni-MNPs. Compared to our previous work[20-24], the recovery protein rate is very low, this is because the number of accessible histidine residues on BHb was 24, the combination between BHb and nickle ions is so strong that 0.1g/ml imidazole cannot totally release the adsorbed BHb. In addition, it is worth noting that as the imidazole solution has strong interaction with the BHb protein the absorbed peak at 406 nm red shifted to 411 nm. The removal efficiency is also observed by a color change of the solution. When the Ni-MNPs are used to remove BHb, the color of a binary protein mixture containing 0.8 mg mL^{-1} BHb and BSA changed from reddish brown to a light color, and the color of 100-fold diluted bovine blood solution changed from red to brown. After the captured BHb on the Ni-MNPs are added to imidazole solution, the elution showed the color of BHb solution.

4. Conclusions and Outlook

In conclusion, we have demonstrated the synthesis of hierarchical nickel anchored on Fe_3O_4@SiO_2 and their successful utilization to remove the abundant proteins(BHb) in bovine blood. The nickel shell play dual role in this work: Firstly, the Ni^{2+} ions at the surface result in the affinity of BHb to the magneitc nanoparticles, thereby allowing them to be selectively and efficiently bound and removed from bovine blood. Secondly, it can make up for the loss of the magnetization of the functional group, which can be easily separated from solution with an applied magnetic field. We believe that the approach presented herein provides a convenient way to bind biomacromolecules to nanomaterials and to produce novel biomedical nanomaterials.

Acknowledgements

The authors are grateful to the financial support by the National Science Foundation of China (No 21305086). The Natural Science Foundation of Shanghai City (13ZR141830), Research

Innovation Program of Shanghai Municipal Education Commission (14YZ138), the Special Scientific Foundation for Outstanding Young Teachers in Shanghai Higher Education Institutions (ZZGJD13016), and Start-up Funding of Shanghai University of Engineering Science.

Notes and references

College of Chemistry and Chemical Engineering, Shanghai University of Engineering Science, Shanghai 201620, China. E-mail: zhangmin@sues.edu.cn; jinglixu2000@163.com

1. A. K. Gupta and M. Gupta, *Biomaterials*, 2005, **26**, 3995.
2. S. Laurent, D. Forge, M. Port, A. Roch, C. Robic, L. V. Elst and R. N. Muller, *Chem. Rev*., 2008, **108**, 2064.
3. H.W. Gu, K. M. Xu, C. J. Xu and B. Xu, *Chem. Commun*.2006, 941.
4. J. H. Gao, H. W. Gu and B. Xu, Acc. *Chem. Res*., 2009, **42**, 1097.
5. D. Hor_ak, M. Babi, H. Mackov and M. J. Bene, *J. Sep. Sci*., 2007,**30**, 1751.
6. I. I. Slowing, L. Juan, V. Escoto, C. W. Wu and V. S. Y. Lin, *Adv. Drug Delivery Rev*., 2008, **60**, 1278.
7. X. G. Luo, S. L. Liu, J. P. Zhou and L. N. Zhang, *J. Mater. Chem*., 2009, **19**, 3538.
8. W. Zhou, N. Yao, G. P. Yao, C. H. Deng, X. M. Zhang and P. Y. Yang, *Chem. Commun*., 2008, 5577.
9. H. M. Chen, D. W. Qi, C. H. Deng, P. Y. Yang and X. M. Zhang, *Proteomics*, 2009, **9**, 380.
10. J. I. Taylor, C. D. Hurst, M. J. Davies, N. Sachsinger and I. J. Bruce, *J. Chromatogr*., A, 2000, **890**, 159.
11. E. J. Woo, K. M. Ponvel, I. S. Ahn, I. S. Ahn and C. H. Lee. J, *Mater. Chem*., 2010, **20**, 1511.
12. C. J. Xu, K. M. Xu, H. W. Gu, X. F. Zhong, Z. H. Guo, R. K. Zheng, X. X. Zhang, and B. Xu, *J. Am. Chem. Soc*., 2004, **126**, 3392.
13. C. J. Xu, K. M. Xu, H. W. Gu, R. K. Zheng, H. Liu, X. X. Zhang, Z. H. Guo, and B. Xu, *J. Am. Chem. Soc*., 2004, **126**, 9938.
14. E. J. Cho, S. Jung, K. Lee, H. J. Lee, K. C. Nam, and H.-J. Bae, *Chem. Commun*., 2010, **46**, 6557.
15. H. Y. Xie, R. Zhen, B. Wang, Y. J. Feng, P. Chen, and J. Hao, *J. Phys. Chem. C*, 2010, **114**, 4825.
16. Z. Liu, M. Li, F. Pu, J. S. Ren, X. J. Yang, and X. G. Qu, *J. Mater. Chem.*, 2012, **22**, 2935.
17. J. Chun, S. W. Seo, G. Y. Jung, and J. Lee, *J. Mater. Chem.*, 2011,**21**, 6713.
18. Z. Liu, M. Li, X. J. Yang, M. L. Yin, J. S. Ren, and X. G. Qu, *Biomaterials*, 2011, **32**, 4683.
19. J. Lee, S. Y. Lee, S. H. Park, H. S. Lee, J. H. Lee, B.-Y. Jeong, S.-E.Park, and J. H. Chang, *J. Mater. Chem. B*, 2013, **1**, 610.
20. M. Zhang, D. Cheng, X. W. He, L. X. Chen, and Y. K. Zhang, *Chem.Asian J*., 2010, 5, 1332.
21. M. Zhang, X. W. He, L. X. Chen, and Y. K. Zhang, J. *Mater. Chem*., 2010, **20**, 10696.
22. M. Zhang, X. W. He, L. X. Chen, and Y. K. Zhang, *Nanotechnology*, 2011, **22**, 65705.
23. G. Q. Jian, Y. X. Liu, X. W. He, L. X. Chen, and Y. K. Zhang, *Nanoscale*, 2012, **4**, 6336.
24. J. L. Cao, X. H. Zhang, X. W. He, L. X. Chen, and Y. K. Zhang, *J. Mater. Chem. B*, 2013, **1**, 3625.
25. Y. T. Zhang, Y. K. Yang, W. F. Ma, J. Guo, Y. Lin, and C. C. Wang. *ACS Appl. Mater. Interface*s 2013, **5**, 2626
26. Y. T. Zhang, D. Li, M. Yu, W. F. Ma, J. Guo, and C. C. Wang. *ACS Appl. Mater. Interfaces* 2014, **5**, 2626.
27. W. J. Fang, X. L. Chen, and N. F. Zheng. *J. Mater. Chem*., 2010, **20**, 8624
28. M. Benelmekki, E. Xuriguera, C. Caparros, E. Rodríguez-Carmona, R. Mendoza, J. L. Corchero, S. Lanceros-Mendez, L.M. Martinez, *J. Colloid Interface Sci* 2012, **365**, 156.
29. Y. Hu, Q. Wang, C. B. Zheng, L. Wu, X. D. Hou and Y. Lv, *Anal. Chem*., 2014, **86**, 842.
30. B.-K. Oh, S. Park, J. E. Millstone, S. W. Lee, K.-B. Lee, C. A. Mirkin, *J. Am. Chem. Soc*. 2006, **128**, 11825.
31. I. S. Lee, N. Lee, J. Park, B. H. Kim, Y.-W. Yi, T. Kim, T. K. Kim, I. H. Lee, S. R. Paik, and T. Hyeon, *J. Am. Chem. Soc*., 2006, **128**, 10658.
32. J. W. Liu, T. Yang, L. Y. Ma, X. W. Chen and J. H. Wang, *Nanotechnology*, 2013, **24**, 505704.
33. W. D. Qu, H. M. Bao, L. Y. Zhang, and G. Chen, *Chem Europ. J.* 2012, **49**, 15746.
34. H. Deng, X. L. Li, Q. Peng, X. Wang, J. P. Chen, and Y. D. Li, *Angew. Chem., Int. Ed*. 2005, **18**, 2842.
35. T. Zhang, J. Ge, Y. Hu, Q. Zhang, S. Aloni, Y. Yin, *Angew. Chem. Int. Ed.*, 2008, **47**, 5806-5811.
36. T. Zhang, Q. Zhang, J. Ge, J. Goebl, M. Sun, Y. Yan, Y.S. Liu, C.L. Chang, *J. Phys. Chem. C*., 2009, **113,** 3168-3175.
37. Y. F. Xu, M. R. Guo, Y. R. Zheng, J. Jiang, S. H. Yu. *Angew. Chem., Int. Ed*. 2013, **52**, 8546.

